

**Inelastic x-ray scattering study of charge-density-wave dynamics in the  $\text{Rb}_{0.3}\text{MoO}_3$  blue bronze**Sylvain Ravy,<sup>1</sup> Herwig Requardt,<sup>2</sup> David Le Bolloc'h,<sup>1</sup> Pascale Foury-Leylekian,<sup>1</sup> Jean-Paul Pouget,<sup>1</sup> Roland Currat,<sup>3</sup> Pierre Monceau,<sup>4,5</sup> and Michael Krisch<sup>2</sup><sup>1</sup>*Laboratoire de Physique des Solides (CNRS-UMR 8502), Université Paris-Sud, Bâtiment 510, 91405 Orsay Cedex, France*<sup>2</sup>*European Synchrotron Radiation Facility, Boîte Postale P 220, 38043 Grenoble Cedex, France*<sup>3</sup>*Institut Laue Langevin, Boîte Postale 156, 38042 Grenoble Cedex, France*<sup>4</sup>*Centre de Recherche sur les Très Basses Températures, CNRS, Boîte Postale 166, 38042 Grenoble Cedex, France*<sup>5</sup>*Laboratoire Léon Brillouin, CEA-CNRS, CE-Saclay, 91191 Gif-sur-Yvette, France*

(Received 10 October 2003; published 18 March 2004)

We present an inelastic x-ray scattering study of the quasi-one-dimensional blue bronze  $\text{Rb}_{0.3}\text{MoO}_3$ . The charge-density-wave (CDW) dynamics is studied as a function of the temperature down to 40 K. At temperature higher than 100 K, the CDW-phase and -amplitude modes are identified, and found consistent with the inelastic neutron scattering measurements. At 40 K, the phason is no longer observed. This is discussed in the framework of current theories on the low-temperature CDW dynamics.

DOI: 10.1103/PhysRevB.69.1151XX

PACS number(s): 63.20.Dj, 71.45.Lr, 72.15.Nj

Charge-density waves (CDW) observed in low-dimensional metals are fascinating examples of electronic crystals.<sup>1,2</sup> They consist in the three-dimensional modulation of the electronic charge density at twice the Fermi wave vector  $2k_F$ , associated with a lattice distortion at the same wave vector. This collective state exhibits very original dynamical properties, such as the capability to transport a nonohmic current. Indeed, due to its incommensurate and charged character, the CDW can be set in motion with respect to the host lattice by applying an electric field larger than a threshold value. The dynamics associated to the CDW above and below the transition temperature  $T_P$  is also an unclarified issue, both on the theoretical and the experimental sides. Above  $T_P$ , the dynamics of the Peierls instability leading to the CDW state is generally described in the framework of weak electron-phonon coupling theory.<sup>3,4</sup> This approach predicts the softening of the phonon mode coupled to the electrons at  $2k_F$  (the Kohn anomaly) and consequently a soft mode-like type of dynamics. Such a Kohn anomaly has been observed in  $\text{K}_2\text{Pt}(\text{CN})_4\text{Br}_{0.3}\cdot 3\text{H}_2\text{O}$  (KCP) (Refs. 5,6) and the blue bronze  $\text{K}_{0.3}\text{MoO}_3$ .<sup>7</sup> However, in  $(\text{TaSe}_4)_2\text{I}$ ,<sup>8</sup> no phonon softening is observed close to the Peierls phase transition, and recent inelastic x-ray scattering (IXS) measurements on  $\text{NbSe}_3$  (Ref. 9) indicate the absence of a Kohn anomaly in this compound as well. These results led the authors of Ref. 9 to reconsider the “strong-coupling” theories,<sup>10</sup> which predict an order-disorder type of dynamics for the Peierls transition, due to the existence of bipolarons above  $T_P$ .

Below  $T_P$ , weak-coupling theory predicts a splitting of the soft mode into two branches, corresponding to CDW-amplitude (amplitudon) and -phase (phason) excitations. In reality once again, the experimental situation is not so simple. Though KCP and blue bronzes<sup>7</sup> exhibit such amplitude and phase modes, these features were observed neither in  $(\text{TaSe}_4)_2\text{I}$  (Ref. 8) nor in  $\text{NbSe}_3$ .<sup>9</sup> Interestingly enough, what makes the CDW state dynamics unique among incommensurate compounds is that the CDW-phase fluctuations induce changes in the electron density which are coupled by long-range Coulomb interactions. Early theories<sup>11</sup> soon recognized that at  $T=0$  K the effect of such interactions

is to transform the acousticlike longitudinal phason mode into an optical one. At finite temperatures however, the quasiparticles excited across the CDW gap screen out the Coulomb interaction and bring back the acoustic character of the phason.<sup>12,13</sup> A dramatic temperature variation of the phase mode is then expected, but has never been evidenced.

The first neutron-scattering investigation of the pretransitional dynamics of the Peierls transition in blue bronze<sup>7</sup> reported the observation of a Kohn anomaly at the wave vector  $2k_F$ , and below  $T_P$ , amplitudon and phason branches. Moreover the study of the phason mode down to 100 K (Ref. 14) revealed a considerable stiffening of the longitudinal phason velocity, confirming the importance of Coulomb forces in CDW dynamics. However, inelastic neutron-scattering (INS) results were limited by the low counting rate, which prevented any measurement at lower temperatures. Motivated by the successful IXS experiments recently performed on  $\text{NbSe}_3$ ,<sup>15</sup> we have carried out similar measurements on the blue bronze  $\text{Rb}_{0.3}\text{MoO}_3$ , from 170 K down to 40 K. Indeed, though limited with respect to energy resolution, IXS provides an excellent  $Q$  resolution, about ten times better than INS, which can be an asset for the study of sharp Kohn anomalies.

Blue bronze  $\text{Rb}_{0.3}\text{MoO}_3$ <sup>2</sup> crystallizes in the monoclinic  $C2/m$  spatial group with the cell parameters  $a=18.54$  Å,  $b=7.556$  Å,  $c=10.035$  Å, and  $\beta=118.5^\circ$ . It consists of clusters of 10  $\text{MoO}_6$  octahedra stacked along the direction [010] and forming layers along the direction [102]. This structure is conveniently analyzed by using the pseudo-orthogonal basis of reciprocal vectors  $\mathbf{b}^*$ , along the direction of the chains,  $2\mathbf{a}^* + \mathbf{c}^* \sim \mathbf{a} + 2\mathbf{c}$ , close to the perpendicular direction within the layer, and  $2\mathbf{a}^* - \mathbf{c}^*$ , perpendicular to the layers. In this framework, typical dimensions of single crystals are  $1 \times 0.5 \times 0.2$  mm<sup>3</sup>.

Electronic band-structure calculations<sup>16</sup> have shown that two quasi-one-dimensional (quasi-1D) bands built from the combination of the Mo 4d orbitals and the O 2p orbitals cross the Fermi level along  $\mathbf{b}^*$ . The rubidium atoms donate three electrons to each  $\text{Mo}_{10}\text{O}_{30}$  cluster, which gives  $2k_F$

$=3/4b^*$ . However, the value of the Fermi wave vector accurately measured by x-ray diffraction experiments is found to have an incommensurate value  $2k_F = 0.748 \pm 0.001b^*$  at 15 K.<sup>17</sup>

Indeed, the periodic lattice distortion (PLD) associated to the charge-density wave gives rise to satellite reflections located at the reciprocal wave vector  $\mathbf{G}_{hkl} + \mathbf{q}_c$  with  $\mathbf{q}_c = (1, 2k_F, 0.5)$ . The phase transition occurs at the critical temperature  $T_p = 183$  K (Ref. 18) whatever the cation, K, or Rb (Ref. 17). The best refinement of the modulated structure<sup>19</sup> has shown that the PLD mainly affects the eight Mo atoms located in the core of the cluster, which are strongly

( $\sim 0.06$  Å) displaced in the [101] direction (transverse polarization). The external Mo atoms and the alkali-metal atoms are slightly displaced in phase in the  $\mathbf{b}^*$  direction (longitudinal polarization), and the oxygen atoms undergo weak displacements.

The experiments have been performed at the IXS beam line ID28 at the European Synchrotron Radiation Facility. We used an incident photon energy  $E_i = 17794$  eV ( $\lambda = 0.6968$  Å) provided by the Si(999)-reflection back-scattering monochromator. Energy scans were performed by varying the monochromator temperature with respect to that of the analyzer crystal (more details can be found in Refs. 20–22). The energy resolution achieved in this configuration was 3.18 meV (full width at half maximum), a value obtained from a fit of a satellite reflection energy scan at 40 K.<sup>23</sup> Attempt to use a better energy resolution (1.5 meV) through Si(11,11,11) reflection at an energy  $E_i = 21747$  eV above the Mo *K* edge led to prohibitive counting times. Let us note that this resolution is about ten times larger than the energy resolution achieved by INS in Ref. 7 (0.3–0.6 meV). In the (999) configuration, most data were taken with counting times never exceeding 10 min/points even at 40 K, leading to sweeping times of less than 3 h to span the  $-20 < E < 20$  meV energy range. For comparison, inelastic neutrons scattering needed counting times twice as long as  $T = 100$  K on a blue bronze sample of exceptional size (5 cm<sup>3</sup>).

A Rb blue bronze sample of standard shape and size was mounted on the cold stage of a closed-cycle helium cryocooler, and was aligned to have its (H,0,L)-reciprocal plane in the horizontal scattering plane. Due to the weak penetration depth (120 μm) of the sample, we used a reflection geometry, which allowed measurements of reflections close to the  $2\mathbf{a}^* - \mathbf{c}^*$  direction. The strongest satellite reflection was found to be at the  $\mathbf{Q}_s = (15, 0.75, -7.5)$  reciprocal position. Entrance slits were set to  $200 \times 500$  μm<sup>2</sup> (H × V), and most of the measurements were performed with an analyser opening of  $10 \times 60$  μm (H × V). With this setting, the half widths at half maximum of the  $\mathbf{Q}_s$  satellite reflection were found to be  $0.0015$  Å<sup>-1</sup>,  $0.0012$  Å<sup>-1</sup>, and  $0.0022$  Å<sup>-1</sup> in the  $\mathbf{b}$ ,  $\mathbf{a} + 2\mathbf{c}$ , and  $2\mathbf{a}^* - \mathbf{c}^*$  directions, respectively.

As the purpose of this experiment was to study the low-temperature CDW dynamics, we directly cooled down the sample to temperatures below  $T_p$ . Energy scans around  $\mathbf{Q}_s$  in the longitudinal direction  $\mathbf{b}^*$  were performed at 170, 100,

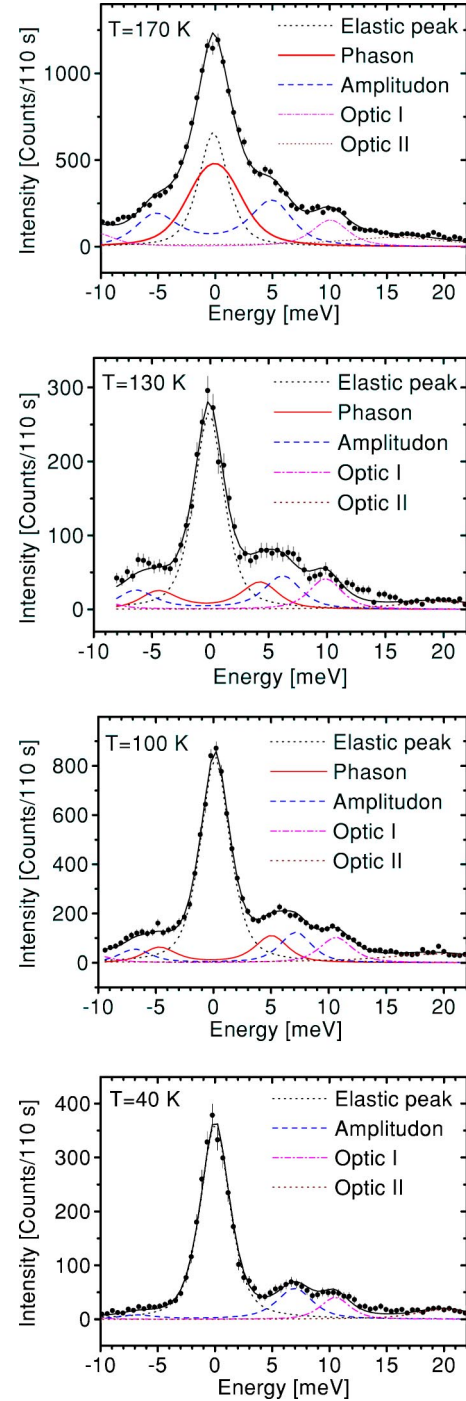


FIG. 1. (Color online) Energy scans at the  $(15.1, 0.75 + 0.02, -7.55)$  position, for four different temperatures. The solid line is the fit by the sum of DHO's functions also indicated in the figure: the dotted, solid, dashed, dot-dashed, and dotted lines are the elastic, phase, amplitude, optic I and II modes, respectively.

40 K, and eventually at 130 K. In order to avoid strong elastic contributions, the scans were taken at the  $\mathbf{Q}_s + 0.05(2\mathbf{a}^* - \mathbf{c}^*) + \delta k\mathbf{b}^*$  positions, i.e., slightly off the satellite position in the transverse direction. Due to the weak dispersion of the CDW-phase mode in this direction (see Fig. 3 in Ref. 8), this procedure is expected not to change the results.

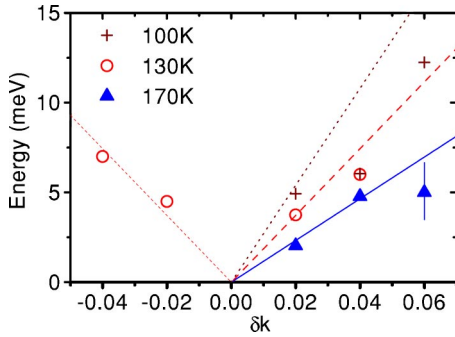


FIG. 2. (Color online) Dispersion curves of the phason mode in the longitudinal  $\mathbf{b}$  direction at 100 K (crosses), 130 K (open circles), and 170 K (triangles). The solid, dashed, and dotted lines represent the slope of the dispersion curves obtained from INS at 170 K, 130 K, and 100 K, respectively.

Typical scans obtained at  $\delta k = 0.02$  are displayed on Fig. 1. The lower intensity of the 130 K scans could be due to a change in the alignment procedure after heating back the sample or to irradiation effects sometimes observed in synchrotron radiation study of blue bronze.<sup>24</sup> The solid lines are fits by a convolution of intrinsic phonon line profiles and the instrumental energy resolution profile. The latter was obtained from a fit by a pseudo-Voigt function of a 40 K energy scan at the exact  $\mathbf{Q}_s$  position, where the elastic peak is largely dominant. The phonon line profiles used were the standard damped harmonic oscillator (DHO) function, with the amplitude, the energy and the damping factor  $\Gamma$  as adjustable parameters. In most of the fits we used the sum of four DHO's, two high-energy modes we called optics I and II at about 10 and 20 meV, the CDW amplitude mode and the phason mode, when necessary. To fit the energy scans, the energy and the damping of the amplitude-mode were constrained to be close to the values obtained from previous INS,<sup>7,14</sup> Raman<sup>25</sup> and ultrafast reflectivity measurements<sup>26</sup> [i.e., of the order of  $E_A = 6.5$  meV and  $\Gamma_A = 2$  meV (Ref. 7)]. Note that at 130 K, the quality of the fit could be improved by adding a mode around 14 meV, but this did not change significantly the results.

The energy values obtained for the phason are indicated on Fig. 2. These values are in good agreement with the dispersion obtained from INS and represented by the lines in Fig. 2 [the phason velocities  $v$  used here are 35, 56, and 81 THz  $\text{\AA}$  (Ref. 27) at 170, 130, and 100 K, respectively— see Fig. 4 of Ref. 14]. The damping values  $\Gamma_p$  at  $\delta k = 0.02$  are indicated in Table I.

Like  $\Gamma_A$ ,  $\Gamma_p$  increases with temperature, a behavior expected due to the increase of the quasiparticles number close to  $T_p$ . It is also noteworthy that although the  $\Gamma_p$  values are found to be smaller than the  $\Gamma_A$  values of Ref. 7, the  $\Gamma_p/\Gamma_A$  ratio is in good agreement with the damping constant ratio  $\tau_A/\tau_p$  obtained by ultrafast reflectivity measurements.<sup>26</sup>

TABLE I. Phason damping values at  $\delta k = 0.02$ .

T	100 K	130 K	170 K
$\Gamma_p(\text{IXS})$	$0.5 \pm 0.4$ meV	$1.2 \pm 0.4$ meV	$1.8 \pm 0.4$ meV

Remarkably, an energy scan was still measurable at 40 K with reasonable counting time, as discussed previously. As expected for such a temperature, the anti-Stokes lines are barely visible but the Stokes lines of the amplitude and the optics modes are still clearly present. As it can be seen in Fig. 1, no extra intensity is now observed between the elastic and the amplitudon peaks, and at higher energy the same quality of fit is achieved with the amplitude and optics modes we used at higher temperatures. This means that no phason mode (at about 4–5 meV) is needed anymore to correctly fit the data at  $T = 40$  K. However, the presence of a weak mode at higher energies would be probably hidden by the other excitations. Nevertheless, the results show for the first time that the phason mode, if present, cannot have the same dispersion as at higher temperature. This is fully consistent with the trend towards Coulomb hardening already observed by INS.<sup>14</sup>

Current theories of CDW dynamics<sup>12,13</sup> predict the phason mode to be acousticlike at high temperature. For large values of the CDW effective mass ratio  $m^*/m$  the phason velocity is given by

$$v_\phi = v_F \sqrt{\frac{m}{m^*}} (1 - f_s(T))^{-1/2}, \quad (1)$$

where  $v_F$  is the Fermi velocity and  $f_s(T)$  is the reduced density of condensed electrons [ $1 - f_s(T)$  is then the reduced density of electron-hole pairs]. It was already shown in Ref. 14 that with  $v_F \sim 1.9 \times 10^5$  m/s,  $m^*/m \sim 150$ , and a  $T = 0$  K CDW gap  $\Delta_0 = 575$  K,<sup>28</sup> the experimental phason velocities above 100 K were well accounted for from Eq. (1).

When the temperature is lowered, the electrons excited across the CDW gap cannot screen the CDW phase deformations anymore, because they are too few and too slow: the phason mode becomes opticlike, with a plasma frequency at  $k = 0$  given by  $\omega_\phi = \sqrt{3/2} \omega_A$ , where  $\omega_A$  is the frequency of the amplitude mode. The crossover between these two regimes is expected to occur at  $T_{cr} \sim 0.17 \Delta_0$ .<sup>13,29</sup> In the case of the blue bronze this temperature can be estimated to be  $T_{cr} \sim 100$  K. According to this calculation, the phason mode is expected to be opticlike at 40 K, with an energy gap equal to  $\sim 8.5$  meV.

It is however an experimental fact that there is no evidence of the phason mode at 40 K. No excitation below about 5 meV is observed anymore and, as mentioned earlier in the text, a line at higher energies could have been difficult to measure because of the vicinity of other lines. This is all the more true since the amplitude of the phason mode is reported to decrease below 100 K (see Fig. 2 in Ref. 26). The combination of these factors could explain why we do not observe the phason line at around 8.5 meV, the energy range where it could be expected according to the previous discussion.

In conclusion, this IXS experiment shows that due to the high brilliance of third generation synchrotron sources it is now possible to measure low-energy excitations in solids by inelastic x-ray scattering, even in cases where neutron-scattering experiments are already challenging. One has to keep in mind however that the analysis of the data would

have been difficult without the prior INS measurements, which allowed us to limit the number of parameters in the fits. The results obtained at 40 K show no indication of a low-energy phason line, which calls for a more precise tem-

perature study of this reciprocal space zone, but confirms the trend towards a Coulomb hardening of the phase-mode previously reported from INS measurements at higher temperatures.

- <sup>1</sup>For reviews on CDW's, see G. Grüner, *Density Waves in Solids* (Addison-Wesley, Reading, MA, 1994); S. Brazovskii, N. Kirova, and P. Monceau, *J. Phys. IV* **12**, Pr9 (2002).
- <sup>2</sup>For reviews on blue bronze properties, see *Low Dimensional Electronic Properties of Molybdenum Bronzes and Oxides*, edited by C. Schlenker (Klüwer Academic, Dordrecht, 1989).
- <sup>3</sup>P.A. Lee, T.M. Rice, and P.W. Anderson, *Solid State Commun.* **14**, 703 (1974).
- <sup>4</sup>E. Tutiš and S. Barišić, *Phys. Rev. B* **43**, 8431 (1991).
- <sup>5</sup>B. Renker, L. Pintschovius, W. Gläser, H. Rietschel, R. Comès, L. Liebert, and W. Drexel, *Phys. Rev. Lett.* **32**, 836 (1974).
- <sup>6</sup>K. Carneiro, G. Shirane, S.A. Werner, and S. Kaiser, *Phys. Rev. B* **13**, 4258 (1976).
- <sup>7</sup>J.-P. Pouget, B. Hennion, C. Escribe-Filippini, and M. Sato, *Phys. Rev. B* **43**, 8421 (1991).
- <sup>8</sup>J.E. Lorenzo, R. Currat, P. Monceau, B. Hennion, H. Berger, and F. Levy, *J. Phys.: Condens. Matter* **10**, 5039 (1998).
- <sup>9</sup>H. Requardt, J.E. Lorenzo, P. Monceau, R. Currat, and M. Krisch, *Phys. Rev. B* **66**, 214303 (2002).
- <sup>10</sup>S. Aubry and P. Quémenerais, in Ref. 2, p. 285.
- <sup>11</sup>P.A. Lee and H. Fukuyama, *Phys. Rev. B* **17**, 542 (1978).
- <sup>12</sup>Y. Nakane and S. Takada, *J. Phys. Soc. Jpn.* **54**, 977 (1985); K.Y.M. Wong and S. Takada, *Phys. Rev. B* **36**, 5476 (1987).
- <sup>13</sup>A. Virosztek and K. Maki, *Phys. Rev. B* **48**, 1368 (1993).
- <sup>14</sup>B. Hennion, J.-P. Pouget, and M. Sato, *Phys. Rev. Lett.* **68**, 2374 (1992).
- <sup>15</sup>H. Requardt, J.E. Lorenzo, R. Danneau, R. Currat, and P. Monceau, *J. Phys. IV* **12**, Pr9-39 (2002).
- <sup>16</sup>M.H. Whangbo and L.F. Schneemeyer, *Inorg. Chem.* **25**, 2424 (1986); J.-L. Mozos, P. Ordejón, and E. Canadell, *Phys. Rev. B* **65**, 233105 (2002).
- <sup>17</sup>J.-P. Pouget, C. Noguera, A.H. Moudden, and R. Moret, *J. Phys. (France)* **46**, 1731 (1985). The deviation of  $2k_F$  from 0.75 is usually believed to be due to residual charged impurities, even in pure materials.
- <sup>18</sup>J.-P. Pouget, S. Kagoshima, C. Schlenker, and J. Marcus, *J. Phys. (France) Lett.* **44**, L113 (1983).
- <sup>19</sup>W.J. Schutte and J.L. De Boer, *Acta Crystallogr., Sect. B: Struct. Sci.* **B49**, 579 (1993).
- <sup>20</sup>F. Sette, G. Ruocco, M. Krisch, C. Masciovecchio, and R. Verbeni, *Phys. Scr.*, **T66**, 48 (1996).
- <sup>21</sup>C. Masciovecchio, U. Bergmann, M.H. Krisch, G. Ruocco, F. Sette, and R. Verbeni, *Nucl. Instrum. Methods Phys. Res. B* **111**, 181 (1996); *ibid.* **117**, 339 (1996).
- <sup>22</sup>R. Verbeni, F. Sette, M.H. Krisch, U. Bergmann, B. Gorges, C. Halcoussis, K. Martel, C. Masciovecchio, J.F. Ribois, G. Ruocco, and H. Sinn, *J. Synchrotron Radiat.* **3**, 62 (1996).
- <sup>23</sup>This energy resolution was found to be narrower than the one usually obtained on ID28 with the same configuration from plexiglass.
- <sup>24</sup>S. Ravy, P. Monceau, A. Ayari, R. Danneau, and H. Requardt, ESRF Report No. HE-844, 2001 (unpublished).
- <sup>25</sup>G. Travaglini, I. Mörke, and P. Waechter, *Solid State Commun.* **45**, 289 (1983).
- <sup>26</sup>J. Demsar, K. Biljaković, and D. Mihailović, *Phys. Rev. Lett.* **83**, 800 (1999).
- <sup>27</sup>The phason velocity  $v$  expressed in THz Å here and in Refs. 7,8, is given by  $v = \nu q$ , where  $\nu$  is the frequency (in THz) and  $q$  the wave vector (in Å<sup>-1</sup>, with the standard  $\mathbf{a} \cdot \mathbf{a}^* = 2\pi$  convention). Care must be taken that in theoretical papers the definition of the mode velocity is  $\omega = v_\phi q$ , hence  $v_\phi = 2\pi v$ .
- <sup>28</sup>This value was obtained from magnetic susceptibility measurements by D.C. Johnston, *Phys. Rev. Lett.* **52**, 2049 (1984); Higher  $\Delta$  values have been obtained, but for the sake of consistency with the INS analysis made in Ref. 7, we have used this value in the following.
- <sup>29</sup>A crude estimation of this crossover temperature can be obtained the following way. The velocity of quasiparticles  $v_T$  is given by the Maxwell-Boltzmann statistics at low temperature, i.e.,  $\frac{1}{2}m_\Delta v_T^2 = \frac{1}{2}k_B T$ , with the effective mass  $m_\Delta^{-1} = 1/\hbar^2 \partial^2 E(k)/\partial k^2 = v_F^2/\Delta$ . As  $v_T = v_F \sqrt{k_B T/\Delta}$  decreases with temperature while the phason velocity given by Eq. (1) increases, the crossover temperature  $T_{cr}$  is obtained when  $v_T \approx v_\phi$ . For the blue bronze this gives  $T_{cr} \sim 100$  K.